Supporting Information for

Model Evaluation of Secondary Chemistry due to Disinfection of Indoor Air with Germicidal Ultraviolet Lamps

Zhe Peng,[1]* Shelly L. Miller,[2] and Jose L. Jimenez[1]*

[1] Cooperative Institute for Research in Environmental Sciences and Department of Chemistry, University of Colorado, Boulder, Colorado 80309, United States

[2] Department of Mechanical Engineering, University of Colorado, Boulder, Colorado 80309, United States

* **Corresponding authors:** Zhe Peng <zhe.peng@colorado.edu>; Jose L. Jimenez <jose.jimenez@colorado.edu>

S1. Oxidation flow reactor mechanism and part of the Regional Atmospheric Chemistry Mechanism (RACM) used in this study

The OFR employs UVC lamps, with the explicit purpose of generating radicals that initiate oxidation reactions. OFR are used extensively in atmospheric chemistry research. A common OFR operation mode ("OFR254") uses 254 nm UV light from filtered mercury lamps to photolyze O_3, through which $O(^1D)$ is generated, which subsequently reacts with water vapor to form OH.[1,2] OFR254 uses the same type of lamps as GUV254 and thus OH is expected to form through the same chemistry. Therefore, all reactions of this inorganic radical chemistry are adopted.[2]

For organic chemistry, the relevant reactions in RACM are adopted. Among major relevant (lumped) species are HC8 (alkanes, alcohols, and esters with relatively fast reaction rate with OH), LIM (limonene), KET (ketones), ALD (aldehydes), OP2 (higher organic peroxides), and ACO3 (acylperoxy radicals). As all inorganic reactions are explicitly included in the OFR mechanism, which is more suitable for the chemistry under GUV, the inorganic part of the RACM mechanism is not used in this study. For simplicity, we generally only include the organic species that are emitted in the case studies in the present work and those that are products of the emitted species in the RACM. Products of a reaction with a yield (stoichiometric coefficient) <0.1 are considered minor and neglected in that reaction. A few reactions (e.g., photolysis of acetic acid (Fig. 1b)) are added to include the chemistry that can occur under UVC irradiation but cannot under UVA and UVB irradiation (only the latter is accounted for by the RACM). All photolysis cross sections are adopted from refs 3,4 when available, otherwise estimated from those of molecules containing the same functional groups according to the framework of Peng et al.[5] All quantum efficiencies for reactant photodissociation except those with available data in refs 3,4 are assumed to be 1, given the high photon energies involved. For GUV222, the photolysis frequencies are calculated using the light flux at that wavelength. Also, as NO_3 concentration is very low in this study, reactions of organics with NO_3 are neglected. All organic reactions used in this study are listed in Table S1.

S2. Lumping of the species in the emission inventory of McDonald et al. into species used in the RACM and initial conditions of the model cases

We lump the (indoor fraction of the) species listed in Table S8 of McDonald et al.[6] into the most similar species in the RACM. The mass fractions of the species in McDonald et al.'s emission inventory in the total VOC are assigned to the mass fractions of the corresponding RACM species. The indoor emission fractions of the RACM species are estimated as a rough average

of those of the lumped species in the McDonald et al. inventory. The resulting indoor mass fractions of the RACM species are renormalized, and with a total VOC of 1.7 mg m^{-3} assumed, the concentrations of individual RACM species can be calculated. The correspondence of the RACM species to those in the McDonald et al. inventory and the estimated indoor emission fractions and normalized mass fractions of the RACM species are shown in Table S2. The only exceptions to this initial VOC concentration estimation are that we assign higher concentrations of 300 ppb to acetone as measured by Price et al.[7] and of 2 ppm to formaldehyde per ref 8.

The atmospheric pressure and temperature in the room are assumed to be 1 atm and 295 K, respectively, with a relative humidity of 37% (water vapor mixing ratio of 1%), and initial NO, HONO, NO_2, and O_3 concentrations of 1, 5, 10, and 10 ppbv, respectively. We assume no NO_x or O_3 emissions indoors, and 5 ppb NO, 20 ppb NO_2, 40 ppb O_3 outdoors. No VOC is assumed to be present in outdoor air, as outdoor VOC levels are typically much lower than indoor ones.[7,9] The O_3 surface loss rate in the absence of chemistry is set to 2.8 h^{-1}, which is typical of residences[10] and is known to be sensitive to occupancy and the indoor surfaces present.

S3. Indoor air exchange rate for the GUV254 case and UV intensity for the GUV222 fixture

The GUV254 fixture in this study has a UV intensity of ~1x10^{14} photons cm^{-2} s^{-1} for the averaged irradiated section area of 4.5 m^2, leading to a virus inactivation rate of ~500 h^{-1} for the irradiated zone. We set an air exchange rate for the irradiated zone at 240 h^{-1} (with the unirradiated zone).[11] As the volume of the irradiated space is 15% of the whole room, the effective virus removal rate for the whole room by GUV254 is ~30 h^{-1} (equivalent ACH) using a SARS-CoV-2 UV inactivation rate of 0.79 cm^2/mJ.[12] Such an equivalent ACH is representative of well-designed indoor GUV applications.[13–15] Air within a modeled indoor air compartment is assumed to be well mixed. Although highly reactive radicals (e.g., OH) may not travel far from the irradiated zone due to short lifetimes,[16] their concentrations can still be averaged over the entire unirradiated space because of their low concentrations and thus the low importance of self- and cross-reactions in their fates.

For the 222 nm UV, we assume its intensity to be uniform all over the room. The same effective virus removal rate as in the occupied unirradiated zone for GUV254 corresponds to a UV intensity of 3.9x10^{12} photons cm^{-2} s^{-1}, with a UV inactivation rate coefficient of 1.42 cm^2 mJ^{-1} for SARS-CoV-2 at 222 nm.[12]

S4. Organic peroxy radical fates in the GUV254 cases

Due to low NO concentration (~30 ppt) at low ventilation, RO_2+NO and RO_2+HO_2 both account for nearly half of the RO_2 bimolecular loss in the irradiated space (Fig. S1). Also, without fast RO_2+NO, RO_2 lifetime is sufficiently long for unimolecular reactions of RO_2 to occur (Fig. S1) as observed previously indoors for similar conditions,[17] although RACM does not include these reactions. In the higher ventilation cases, NO, though still consumed by the photochemistry, is much higher due to a stronger replenishment from outdoor air and can dominate the RO_2 bimolecular fate (Fig. S1).

S5. Sensitivity GUV cases with high VOC emissions

These sensitivity cases for GUV254 and GUV222 have x10 indoor VOC emissions as an example of a very polluted indoor space. All other settings for this case are the same as the corresponding GUV254 and GUV222 cases with low ventilation. Compared to the standard low-ventilation GUV cases, the steady-state concentrations of gas-phase organic products and SOA are ~5-10 times higher. O_3 is lower because of stronger limonene ozonolysis. Relative to a no-UV case with x10 VOC emissions, SOA formation enhancement due to GUV is ~4 μg m^{-3} in the GUV254 sensitivity case. In the GUV222 sensitivity case, GUV-enhanced SOA formation is ~60 μg m^{-3}, largely due to limonene ozonolysis promoted by GUV222-induced O_3 production. These SOA enhancements account for similar fractions of total SOA formation as in the standard low-ventilation GUV254 and GUV222 cases.

S6. Sensitivity GUV cases with wildfire smoke in the outdoor air

These sensitivity cases for GUV254 and GUV222 have a highly polluted outdoor air composition. We assumed that in the outdoor air there is wildfire smoke with an OA concentration of 200 μg m^{-3}, which is an upper limit for wildfire smoke in urban areas in the Western US.[18] The fractions of gas-phase organic species in the total organic carbon are estimated based on the wildfire plume organic species concentrations reported by Heald et al.[19] These species are lumped with the most similar species in the chemical mechanism used in this study. The NO concentration is estimated based on the emission factors reported by Urbanski.[20]

Compared to the base low-ventilation GUV254 and GUV222 cases, all changes in the stable organic product concentrations are within 20%, except for those with high concentrations outdoors, e.g., OA and PAN. The increases in the concentrations of these species are

dominantly due to ventilation. At higher ventilation rates, the increases in the indoor concentrations of even more species (e.g., NO and ketones) are dominated by the ventilation.

References:

(1) Peng, Z.; Day, D. A.; Stark, H.; Li, R.; Lee-Taylor, J.; Palm, B. B.; Brune, W. H.; Jimenez, J. L. HOx Radical Chemistry in Oxidation Flow Reactors with Low-Pressure Mercury Lamps Systematically Examined by Modeling. *Atmospheric Measurement Techniques* **2015**, *8* (11), 4863–4890.

(2) Peng, Z.; Jimenez, J. L. Radical Chemistry in Oxidation Flow Reactors for Atmospheric Chemistry Research. *Chem. Soc. Rev.* **2020**, *49* (9), 2570–2616.

(3) Burkholder, J. B.; Sander, S. P.; Abbatt, J.; Barker, J. R.; Huie, R. E.; Kolb, C. E.; Kurylo, M. J.; Orkin, V. L.; Wilmouth, D. M.; Wine, P. H. *Chemical Kinetics and Photochemical Data for Use in Atmospheric Studies: Evaluation Number 18*; Jet Propulsion Laboratory: Pasadena, CA, USA, 2015.

(4) Keller-Rudek, H.; Moortgat, G. K.; Sander, R.; Sörensen, R. *The MPI-Mainz UV/VIS Spectral Atlas of Gaseous Molecules of Atmospheric Interest*. http://satellite.mpic.de/spectral_atlas (accessed 2022-02-10).

(5) Peng, Z.; Lee-Taylor, J.; Stark, H.; Orlando, J. J.; Aumont, B.; Jimenez, J. L. Evolution of OH Reactivity in NO-Free Volatile Organic Compound Photooxidation Investigated by the Fully Explicit GECKO-A Model. *Atmos. Chem. Phys.* **2021**, *21* (19), 14649–14669.

(6) McDonald, B. C.; de Gouw, J. A.; Gilman, J. B.; Jathar, S. H.; Akherati, A.; Cappa, C. D.; Jimenez1, J. L.; Lee-Taylor, J.; Hayes, P. L.; McKeen, S. A.; Cui, Y. Y.; Kim, S.-W.; Gentner, D. R.; Isaacman-VanWertz, G.; Goldstein, A. H.; Harley, R. A.; Frost, G. J.; Roberts, J. M.; Ryerson, T. B.; Trainer, M. Volatile Chemical Products Emerging as Largest Petrochemical Source of Urban Organic Emissions. *Science* **2018**, *359* (6377), 760–764.

(7) Price, D. J.; Day, D. A.; Pagonis, D.; Stark, H.; Algrim, L. B.; Handschy, A. V.; Liu, S.; Krechmer, J. E.; Miller, S. L.; Hunter, J. F.; de Gouw, J. A.; Ziemann, P. J.; Jimenez, J. L. Budgets of Organic Carbon Composition and Oxidation in Indoor Air. *Environ. Sci. Technol.* **2019**. https://doi.org/10.1021/acs.est.9b04689.

(8) Logue, J. M.; McKone, T. E.; Sherman, M. H.; Singer, B. C. Hazard Assessment of Chemical Air Contaminants Measured in Residences. *Indoor Air* **2011**, *21* (2), 92–109.

(9) Mattila, J. M.; Arata, C.; Abeleira, A.; Zhou, Y.; Wang, C.; Katz, E. F.; Goldstein, A. H.; Abbatt, J. P. D.; DeCarlo, P. F.; Vance, M. E.; Farmer, D. K. Contrasting Chemical Complexity and the Reactive Organic Carbon Budget of Indoor and Outdoor Air. *Environmental Science & Technology*. 2022, pp 109–118. https://doi.org/10.1021/acs.est.1c03915.

(10) Lee, K.; Vallarino, J.; Dumyahn, T.; Ozkaynak, H.; Spengler, J. D. Ozone Decay Rates in Residences. *J. Air Waste Manage. Assoc.* **1999**, *49* (10), 1238–1244.

(11) Nicas, M.; Miller, S. L. A Multi-Zone Model Evaluation of the Efficacy of Upper-Room Air Ultraviolet Germicidal Irradiation. *Appl. Occup. Environ. Hyg.* **1999**, *14* (5), 317–328.

(12) Ma, B.; Gundy, P. M.; Gerba, C. P.; Sobsey, M. D.; Linden, K. G. UV Inactivation of SARS-CoV-2 across the UVC Spectrum: KrCl* Excimer, Mercury-Vapor, and Light-Emitting-Diode (LED) Sources. *Appl. Environ. Microbiol.* **2021**, *87* (22), e0153221.

(13) Xu, P.; Kujundzic, E.; Peccia, J.; Schafer, M. P.; Moss, G.; Hernandez, M.; Miller, S. L. Impact of Environmental Factors on Efficacy of Upper-Room Air Ultraviolet Germicidal

Irradiation for Inactivating Airborne Mycobacteria. *Environ. Sci. Technol.* **2005**, *39* (24), 9656–9664.
(14) Xu, P.; Peccia, J.; Fabian, P.; Martyny, J. W.; Fennelly, K. P.; Hernandez, M.; Miller, S. L. Efficacy of Ultraviolet Germicidal Irradiation of Upper-Room Air in Inactivating Airborne Bacterial Spores and Mycobacteria in Full-Scale Studies. *Atmos. Environ.* **2003**, *37* (3), 405–419.
(15) Nardell, E. A. Air Disinfection for Airborne Infection Control with a Focus on COVID-19: Why Germicidal UV Is Essential. *Photochem. Photobiol.* **2021**, *97* (3), 493–497.
(16) Lakey, P. S. J.; Won, Y.; Shaw, D.; Østerstrøm, F. F.; Mattila, J.; Reidy, E.; Bottorff, B.; Rosales, C.; Wang, C.; Ampollini, L.; Zhou, S.; Novoselac, A.; Kahan, T. F.; DeCarlo, P. F.; Abbatt, J. P. D.; Stevens, P. S.; Farmer, D. K.; Carslaw, N.; Rim, D.; Shiraiwa, M. Spatial and Temporal Scales of Variability for Indoor Air Constituents. *Communications Chemistry* **2021**, *4* (1), 110.
(17) Pagonis, D.; Algrim, L. B.; Price, D. J.; Day, D. A.; Handschy, A. V.; Stark, H.; Miller, S. L.; de Gouw, J. A.; Jimenez, J. L.; Ziemann, P. J. Autoxidation of Limonene Emitted in a University Art Museum. *Environ. Sci. Technol. Lett.* **2019**, *6* (9), 520–524.
(18) O'Dell, K.; Ford, B.; Burkhardt, J.; Magzamen, S.; Anenberg, S. C.; Bayham, J.; Fischer, E. V.; Pierce, J. R. Outside in: The Relationship between Indoor and Outdoor Particulate Air Quality during Wildfire Smoke Events in Western US Cities. *Environ. Res.: Health* **2022**. https://doi.org/10.1088/2752-5309/ac7d69.
(19) Heald, C. L.; Goldstein, A. H.; Allan, J. D.; Aiken, A. C.; Apel, E.; Atlas, E. L.; Baker, A. K.; Bates, T. S.; Beyersdorf, A. J.; Blake, D. R.; Others. Total Observed Organic Carbon (TOOC) in the Atmosphere: A Synthesis of North American Observations. *Atmos. Chem. Phys.* **2008**, *8* (7), 2007–2025.
(20) Urbanski, S. Wildland Fire Emissions, Carbon, and Climate: Emission Factors. *For. Ecol. Manage.* **2014**, *317*, 51–60.
(21) Stockwell, W. R.; Kirchner, F.; Kuhn, M.; Seefeld, S. A New Mechanism for Regional Atmospheric Chemistry Modeling. *J. Geophys. Res.* **1997**, *102* (D22), 25847–25879.
(22) Peng, Z.; Jimenez, J. L. KinSim: A Research-Grade, User-Friendly, Visual Kinetics Simulator for Chemical-Kinetics and Environmental-Chemistry Teaching. *J. Chem. Educ.* **2019**, *96* (4), 806–811.
(23) Saathoff, H.; Naumann, K.-H.; Möhler, O.; Jonsson, Å. M.; Hallquist, M.; Kiendler-Scharr, A.; Mentel, T. F.; Tillmann, R.; Schurath, U. Temperature Dependence of Yields of Secondary Organic Aerosols from the Ozonolysis of α-Pinene and Limonene. *Atmos. Chem. Phys.* **2009**, *9* (5), 1551–1577.
(24) Peng, Z.; Lee-Taylor, J.; Orlando, J. J.; Tyndall, G. S.; Jimenez, J. L. Organic Peroxy Radical Chemistry in Oxidation Flow Reactors and Environmental Chambers and Their Atmospheric Relevance. *Atmos. Chem. Phys.* **2019**, *19* (2), 813–834.
(25) Praske, E.; Otkjær, R. V.; Crounse, J. D.; Hethcox, J. C.; Stoltz, B. M.; Kjaergaard, H. G.; Wennberg, P. O. Atmospheric Autoxidation Is Increasingly Important in Urban and Suburban North America. *Proceedings of the National Academy of Sciences* **2018**, *115* (1), 64–69.
(26) Orlando, J. J.; Tyndall, G. S. Laboratory Studies of Organic Peroxy Radical Chemistry: An Overview with Emphasis on Recent Issues of Atmospheric Significance. *Chem. Soc. Rev.* **2012**, *41* (19), 6294–6317.

Table S1. Organic (a) thermal and (b) photolytic reactions in the chemical scheme in this study. See Table 1 of Stockwell et al.[21] for the species names that are not common names or chemical formulas. Note that some reactions with the same reactants are divided into multiple reactions to fit the 3-product requirement of KinSim.[22]

(a)

Reactants		Products			Rate coefficient (cm^3 $molecules^{-1}$ s^{-1} or s^{-1})
CH3OO	HO2	CH3OOH			5.20E-12
CH3OO	NO	HCHO	NO2		7.60E-12
ACO3	NO	CH3OO	NO2		2.00E-11
CH3OOH	OH	CH3OO	H2O		7.40E-12
HCHO	OH	CO	H2O	HO2	8.50E-12
CO	OH	CO2	HO2		2.10E-13
CH3OO	CH3OO	2 HCHO	2 HO2		1.23E-13
CH3OO	CH3OO	HCHO	CH3OH		2.28E-13
CH3OH	OH	HCHO	HO2	H2O	9.10E-13
ACO3	NO2	PAN			8.66E-12
ACO3	HO2	CH3CO3H			5.60E-12
ACO3	HO2	CH3COOH	O3		2.80E-12
ACO3	HO2	CH3OO	OH		5.60E-12
LIM	OH	LIMP			1.71E-10
LIMP	NO	1.3 HO2	0.8 MACR	0.5 OLI	2.00E-12
LIMP	NO	0.5 HCHO	0.7 ONIT	1.3 NO2	2.00E-12
LIMP	HO2	OP2			1.50E-11
LIMP	CH3OO	2.8 HCHO	1.2 MACR	0.8 OLI	1.92E-13
LIMP	CH3OO	4 HO2			1.92E-13

LIMP	ACO3	1.2 MACR	0.8 HCHO	0.8 OLI	4.82E-12
LIMP	ACO3	2 HO2	2 CH3OO		4.82E-12
MACR	OH	0.51 ACO3	0.41 HKET	0.49 HO2	3.35E-11
MACR	O3	1.2 HCHO	1.8 MGLY		3.80E-19
MACR	O3	0.39 CH3COOH	0.66 HCOOH	0.21 OH	3.80E-19
MACR	O3	0.87 HO2	0.39 OP2	0.39 ACO3	3.80E-19
LIM	O3	0.92 OLT	0.32 ETHP	0.84 KETP	1.00E-16
LIM	O3	1.7 OH	0.2 HO2	1.58 MACR	1.00E-16
OLI	OH	OLIP			7.12E-11
OLI	O3	1.98 ALD	0.32 KET	0.28 CH3COOH	1.29E-16
OLI	O3	0.44 HO2	1.26 OH	0.46 CH3OO	1.29E-16
OLIP	NO	2 HO2	2 NO2		2.00E-12
OLIP	NO	3.42 ALD	0.58 KET		2.00E-12
OLIP	HO2	OP2			1.00E-11
OLIP	CH3OO	1.51 HCHO	2 HO2		4.93E-13
OLIP	CH3OO	1.864 ALD	0.626 KET		4.93E-13
OLIP	ACO3	1.882 ALD	1.138 KET	1.02 HO2	3.32E-12
OLIP	ACO3	1.02 CH3OO	0.98 CH3COOH		3.32E-12
ONIT	OH	HC3P	NO2		2.22E-12
OP2	OH	0.44 HC3P	0.41 KET	0.49 OH	6.43E-12
HKET	OH	HO2	MGLY		3.00E-12
MGLY	OH	ACO3			1.72E-11
OLT	OH	OLTP			3.06E-11

OLTP	NO	1.88 ALD	0.12 KET		2.00E-12
OLTP	NO	2 HCHO	2 HO2	2 NO2	2.00E-12
OLTP	HO2	OP2			1.30E-11
OLTP	CH3OO	1.25 HCHO	HO2	0.669 ALD	1.57E-12
ETHP	NO	ALD	HO2	NO2	8.70E-12
ETHP	HO2	OP2			7.86E-12
ETHP	CH3OO	0.75 HCHO	HO2	0.75 ALD	2.01E-13
ETHP	ACO3	2 ALD	HO2		1.05E-12
ETHP	ACO3	CH3OO	CH3COOH		1.05E-12
KETP	NO	1.08 MGLY	0.92 ALD	0.46 ACO3	2.00E-12
KETP	NO	1.54 HO2	2 NO2		2.00E-12
KETP	HO2	OP2			9.02E-12
KETP	CH3OO	1.5 HCHO	1.76 HO2	0.8 MGLY	1.90E-12
KETP	CH3OO	0.6 ALD	0.6 HKET	0.24 ACO3	1.90E-12
KETP	ACO3	1.62 MGLY	1.05 ALD	0.33 KET	1.67E-12
KETP	ACO3	0.36 ACO3	1.14 HO2	1.5 CH3OO	1.67E-12
KETP	ACO3	1.5 CH3COOH			1.67E-12
ALD	OH	ACO3			1.69E-11
KET	OH	KETP			6.87E-13
HC3P	NO	0.466 ALD	1.246 KET	1.484 HO2	2.00E-12
HC3P	NO	0.3 CH3OO	1.882 NO2		2.00E-12
HC3P	HO2	OP2			1.30E-11
HC3P	CH3OO	0.81 HCHO	0.992 HO2	0.58 ALD	4.02E-13
HC3P	ACO3	1.448 ALD	0.254 KET	0.976 HO2	1.62E-12

HC3P	ACO3	1.016 CH3OO	0.998 CH3COOH		1.62E-12
ACO3	ACO3	2 CH3OO			1.66E-11
ACO3	CH3CO3	2 CH3OO			1.66E-11
ACO3	CH3OO	HCHO	HO2	CH3OO	7.33E-12
ACO3	CH3OO	HCHO	CH3COOH		1.22E-12
HC3	OH	0.583 HC3P	0.381 HO2	0.335 ALD	2.20E-12
HC8	OH	0.951 HC8P			1.08E-11
HC8P	NO	0.3 ALD	1.282 KET	0.266 ETHP	2.00E-12
HC8P	NO	0.522 ONIT	1.478 NO2	1.212 HO2	2.00E-12
TOL	OH	TOLP			5.96E-12
XYL	OH	XYLP			2.40E-11
HC8P	HO2	OP2			1.30E-11
HC8P	CH3OO	1.506 HCHO	1.986 HO2		1.82E-13
HC8P	CH3OO	0.822 ALD	0.838 KET		1.82E-13
HC8P	ACO3	0.994 ALD	1.162 KET		1.22E-12
HC8P	ACO3	1.014 CH3OO	0.99 CH3COOH		1.22E-12
TOLP	NO	1.9 NO2	1.9 HO2		2.00E-12
TOLP	NO	1.3 MGLY	2.4 GLY	DCB	2.00E-12
XYLP	NO	1.9 NO2	1.9 HO2		2.00E-12
XYLP	NO	1.2 MGLY	0.7 GLY	1.9 DCB	2.00E-12
TOLP	HO2	OP2			1.01E-11
XYLP	HO2	OP2			1.01E-11
TOLP	CH3OO	2 HCHO	2 HO2	2 DCB	1.92E-13

TOLP	CH3OO	0.7 MGLY	1.3 GLY		1.92E-13
XYLP	CH3OO	2 HCHO	2 HO2	2 DCB	1.92E-13
XYLP	CH3OO	1.26 MGLY	0.74 GLY		1.92E-13
TOLP	ACO3	2 CH3OO	2 HO2	2 DCB	4.82E-12
TOLP	ACO3	0.7 MGLY	1.3 GLY		4.82E-12
XYLP	CH3OO	2 HCHO	2 HO2	2 DCB	4.82E-12
XYLP	CH3OO	1.26 MGLY	0.74 GLY		4.82E-12
GLY	OH	HO2			1.14E-11
CH3CH2OH	OH	ALD	HO2		3.20E-12
iPrOH	OH	acetone	HO2		5.10E-12
PAN		ACO3	NO2		0.00033

(b)

Reactants / UV photons		Products			Cross section (cm^2)
O2	UV at 222 nm	2 O(3P)			4.09E-24
acetone		CO	2 CH3OO		1.03E-21
acetone		ACO3	CH3OO		1.91E-21
CH3OOH		HCHO	OH		1.41E-19
HCHO		0.61 HO2	0.7 CO	0.495 H2	1.80E-22
PAN		ACO3	NO2		6.22E-19
PAN		CH3OO	NO3		1.55E-19
CH3CO3H		CH3OO	OH		1.60E-19
MACR		ACO3	HCHO	HO2	1.40E-18
ONIT		0.4 ALD	1.6 KET		5.00E-19

ONIT		2 HO2	2 NO2		5.00E-19
OP2		ALD	HO2	OH	1.41E-19
HKET		HCHO	HO2	ACO3	2.94E-21
MGLY		HO2	ACO3		1.43E-20
CH3COOH		ACO3	OH		5.09E-20
CH3COOH		CH3OO	HO2		4.34E-20
HCOOH		OH	HO2		1.24E-19
ALD		CH3OO	HO2		6.50E-22
KET		ETHP	ACO3		2.94E-21
GLY		0.45 HCHO	0.8 HO2		6.16E-21
acetone	UV at 254 nm	CO	2 CH3OO		1.06E-20
acetone		ACO3	CH3OO		1.95E-20
CH3OOH		HCHO	OH		3.40E-20
HCHO		0.61 HO2	0.7 CO	0.495 H2	3.69E-21
PAN		ACO3	NO2		8.00E-20
PAN		CH3OO	NO3		2.00E-20
CH3CO3H		CH3OO	OH		2.42E-20
MACR		ACO3	HCHO	HO2	1.79E-21
ONIT		0.4 ALD	1.6 KET		2.50E-20
ONIT		2 HO2	2 NO2		2.50E-20
OP2		ALD	HO2	OH	3.40E-20
HKET		HCHO	HO2	ACO3	4.98E-20
MGLY		HO2	ACO3		2.76E-20

ALD		CH3OO	HO2		1.57E-20
KET		ETHP	ACO3		3.01E-20
GLY		0.45 HCHO	0.8 HO2		1.41E-20

Table S2. Correspondences of the RACM species to those in the McDonald et al.[6] emission inventory and estimated indoor emission fractions and normalized mass fractions of the RACM species.

RACM species	RACM species molar weight (g mol^{-1})	Corresponding species in the McDonald et al. inventory	Estimated indoor emission fraction	Normalized mass fraction
HC3	44	Straight-chain and branched alkanes up to C5	17%	4.2%
HC8	114	C6 and higher straight-chain and branched alkanes and all cycloalkanes	58%	22.7%
TOL	92	toluene	37%	1.5%
XYL	106	All higher aromatics	14%	1.3%
LIM	136	All alkenes/cycloalkenes	93%	9.5%
CH_3CH_2OH	46	ethanol	87%	27.3%
iPrOH	60	i-propyl alcohol	91%	16.8%
KET	72	All other oxygenated VOCs	22%	16.8%

Table S3. Concentrations of the major (types of) species in the irradiated and unirradiated zones and ratios between them in the GUV254 cases at different ventilation rates.

GUV254 cases	Species (concentration unit)	Concentration in the irradiated zone	Concentration in the unirradiated zone	Ratio between the concentrations in the irradiated and unirradiated zones
Low ventilation	SARS-CoV-2 (quanta)	1.89E-01	6.14E-01	0.31
	O_3 (molecules cm^{-3})	9.37E+10	9.29E+10	1.01
	OH (molecules cm^{-3})	4.87E+04	2.33E+04	2.09
	HO_2 (molecules cm^{-3})	8.00E+08	7.52E+08	1.06
	NO (molecules cm^{-3})	6.90E+08	6.93E+08	1.00
	Aldehydes except formaldehyde (molecules cm^{-3})	4.11E+10	4.11E+10	1.00
	Ketones except acetone (molecules cm^{-3})	2.26E+12	2.26E+12	1.00
	Peroxides (molecules cm^{-3})	1.21E+11	1.21E+11	1.00
	Organic nitrates (molecules cm^{-3})	4.70E+10	4.67E+10	1.01
	Alkylperoxys (molecules cm^{-3})	1.63E+09	1.18E+09	1.39
	Acylperoxys (molecules cm^{-3})	4.78E+06	8.48E+04	56.36
	SOA (μg m^{-3})	9.59E+00	9.59E+00	1.00
Medium ventilation	SARS-CoV-2 (quanta)	1.73E-01	5.64E-01	0.31
	O_3 (molecules cm^{-3})	5.02E+11	4.98E+11	1.01
	OH (molecules cm^{-3})	1.56E+06	4.75E+05	3.27
	HO_2 (molecules cm^{-3})	5.43E+08	4.49E+08	1.21
	NO (molecules cm^{-3})	6.68E+09	6.76E+09	0.99
	Aldehydes except formaldehyde (molecules cm^{-3})	5.84E+09	5.80E+09	1.01
	Ketones except acetone	2.28E+11	2.28E+11	1.00

	(molecules cm^{-3})			
	Peroxides (molecules cm^{-3})	3.25E+09	3.23E+09	1.01
	Organic nitrates (molecules cm^{-3})	3.36E+09	3.32E+09	1.01
	Alkylperoxys (molecules cm^{-3})	4.42E+08	3.00E+08	1.48
	Acylperoxys (molecules cm^{-3})	5.88E+05	1.10E+05	5.37
	SOA (μg m^{-3})	8.05E-01	7.98E-01	1.01
High ventilation	SARS-CoV-2 (quanta)	1.45E-01	4.77E-01	0.30
	O_3 (molecules cm^{-3})	7.08E+11	7.02E+11	1.01
	OH (molecules cm^{-3})	4.74E+06	7.97E+05	5.95
	HO_2 (molecules cm^{-3})	2.27E+08	1.26E+08	1.80
	NO (molecules cm^{-3})	1.78E+10	1.80E+10	0.99
	Aldehydes except formaldehyde (molecules cm^{-3})	1.27E+09	1.23E+09	1.03
	Ketones except acetone (molecules cm^{-3})	7.61E+10	7.61E+10	1.00
	Peroxides (molecules cm^{-3})	1.19E+08	1.12E+08	1.07
	Organic nitrates (molecules cm^{-3})	8.99E+08	8.59E+08	1.05
	Alkylperoxys (molecules cm^{-3})	1.96E+08	8.08E+07	2.42
	Acylperoxys (molecules cm^{-3})	2.31E+05	5.61E+04	4.11
	SOA (μg m^{-3})	1.75E-01	1.67E-01	1.05

Table S4. Mass yields of secondary organic aerosol produced through several volatile organic compound oxidation pathways.

VOC + oxidant	Mass yield	Source
LIM + O_3	20%	Estimated based on ref 23
LIM + OH	13%	Ref 6
HC8 + OH	10%	Rough average of yields for corresponding species in the inventory of ref 6
KET + OH	5%	Rough average of yields for corresponding species in the inventory of ref 6
TOL + OH	9%	Ref 6
XYL + OH	4.9%	Ref 6

(a)

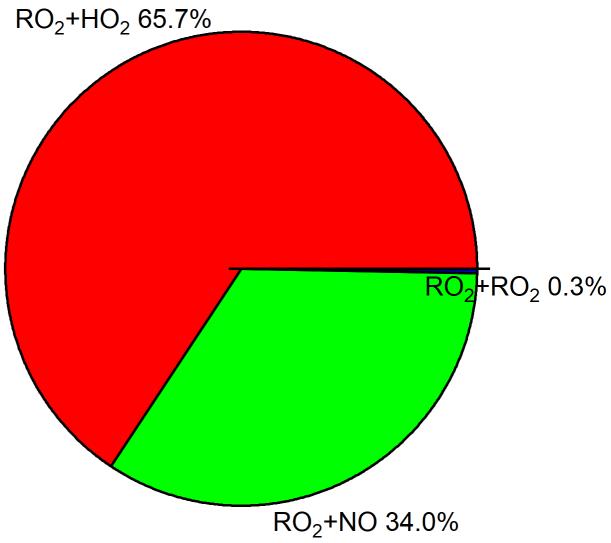
RO2+HO2 65.7%
RO2+RO2 0.3%
RO2+NO 34.0%

(b)

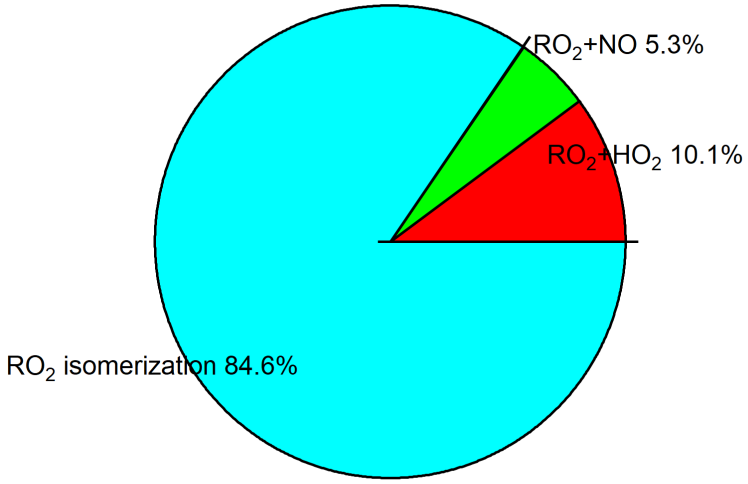
RO2+NO 5.3%
RO2+HO2 10.1%
RO2 isomerization 84.6%

(c)

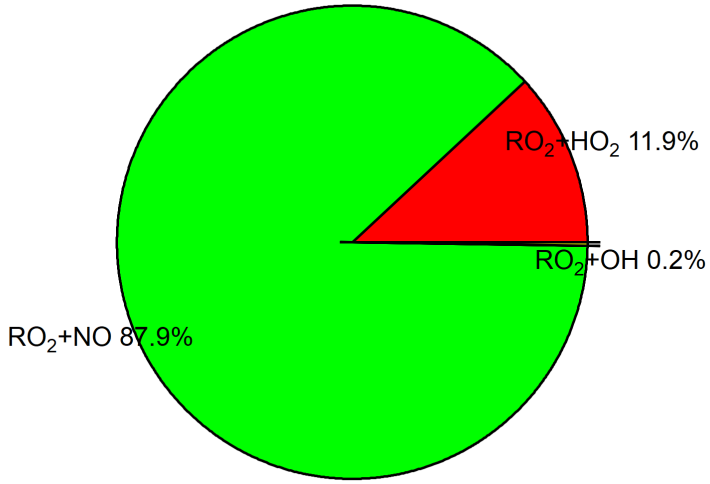

(d)

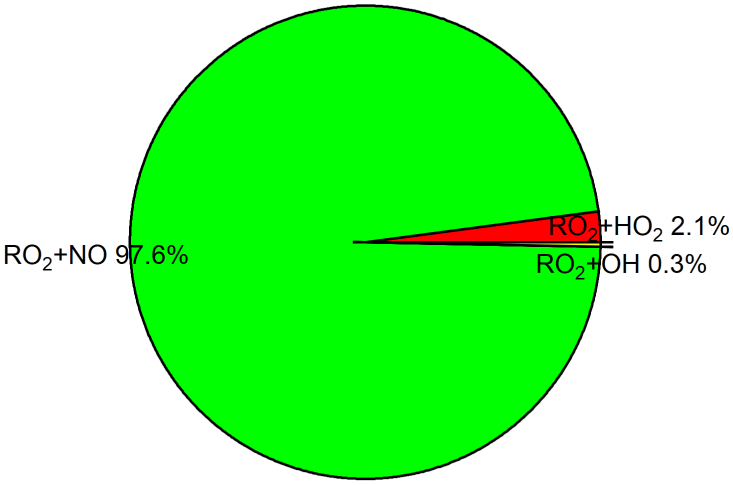

Figure S1. Alkyl RO_2 fate estimated per Peng et al.:[24] (a) bimolecular fate and (b) fate including unimolecular isomerization in the low-ventilation GUV254 case, and bimolecular fate in the (c) medium- and (d) high-ventilation GUV254 cases. RO_2 unimolecular isomerization rate coefficient is assumed to be 0.1 s^{-1}, typical for oxygenated VOCs.[25] "RO_2+RO_2" denotes the reaction between an alkyl RO_2 and an acyl RO_2, with a rate coefficient assumed to be $1x10^{-11}$ cm^3 $molecule^{-1}$ s^{-1}.[26]